Measurement of Structured Microbial Population Dynamics by Flow Microfluorometry

JAMES E. BAILEY
JILA FAZEL-MADJLESSI
DONALD N. McQUITTY
L. Y. LEE
and
JAMES A. ORO

University of Houston
Houston, Texas 77004

Commercial microbiological processes frequently contain dispersed microorganisms which are heterogeneous in their age, size, and composition. Relative protein and nucleic acid contents of individual bacteria in *Bacillus subtilis* submerged cultures have been measured experimentally using laser flow microfluorometry. Marginal and joint population composition density data and their complex patterns of evolution during batch growth provide an impetus and emerging basis for a new generation of potentially robust mathematical models of microbial systems.

SCOPE

Available kinetic models for microbiological processes are often inadequate for design of biological reactors with flow and mixing patterns different from those encountered in the kinetic experiments. It has been recognized for some time (Fredrickson et al., 1970) that this failure is a consequence of two types of aggregation commonly employed in modeling microbial systems. The first is use of a small number of state variables, often only one (cell number or cell mass concentration), to characterize the biophase. The other is treating the dispersed suspension of microorganisms, with their individual differences in age, size, composition, and stage in life cycle, as a homogeneously distributed and uniform solute.

The general structure of a broad class of population balance microbiological process models including an arbitrary number of components for the biological phase as well as explicit recognition of potential individual differences among suspended cells has already been enunciated (Fredrickson et al., 1967). Development of specific models which capitalize on this potential generality has been limited by experimental access to the requisite information for model identification and verification.

Multicomponent measurements of microbial cell composition have previously been practically possible only for samples containing large numbers of cells. Such methods inherently provide only population-average results rather than composition information on the diverse collection of individual cells present in the cell population. Individual cell data have heretofore been limited to size measurement via the Coulter principle.

In this work, a new experimental technique, laser flow microfluorometry, has been employed to examine the compositions of individual bacterial cells grown in submerged culture and to observe thereby the dynamics of microbial population composition distributions.

CONCLUSIONS AND SIGNIFICANCE

It has been shown that with careful signal processing and instrument alignment, laser flow microfluorometry is capable of measuring fluorescence from stained protein and nucleic acid in individual bacterial cells. Distributions of protein and nucleic acid in the cell population show significant variation over the course of a batch fermentation. Substantial detail on the dynamics of culture subpopulations, which in this case include spores, vegetative cells, and chains of vegetative bacteria, can be readily discerned from the FMF information. Simultaneous two-color fluorescence measurements also have been successfully obtained for this bacterial fermentation. The resulting two-component composition data are superior to one-color fluorescence information in that, in addition to greater information on the structure of the microbial population, enhanced sensitivity is obtained for low level fluorescence signals.

Observed changes in composition distributions with time during batch growth are quite complicated (see Figures 3 through 5) and illustrate the need to include multiple composition variables when analyzing the microbial population. One observation which dictates this requirement is the lack of any apparent correlation between protein and nucleic acid distributions over the course of the batch growth cycle. The experimentally determined composition distributions and their changes are substantially more complex than volume or mass distributions and their dynamics as predicted in previous solutions of population balance models for microbial growth.

This work introduces a powerful new experimental approach for study of microbial processes and further illustrates the usefulness of the technique in elucidating the population dynamics of a batch bacterial fermentation. Flow microfluorometry provides the experimental capability necessary for development of microbial population balance models which include cellular composition variables. Models of this class may well provide a more general basis for analysis and design of microbiological processes than presently available methods.

Correspondence concerning this paper should be addressed to James E. Bailey.

0001-1541-78-1141-0569-$01.05.

Since the first observations of batch growth patterns near the turn of the century (for example, Ward, 1895), microbiologists have investigated the factors controlling microbial nutrient utilization, growth, and product formation. Biochemical engineers have for the past 20 yr joined in this quest, seeking reliable kinetic expressions and models for development, scale-up, and control of fermentation processes (for example, Gaden, 1955; Fredrickson, 1977). With progress in these endeavors have come new insights into cellular function, as biochemists have revealed the inherent complexities of cellular regulation and control. Studies of microbial metabolism and subsets of the overall cellular reaction system have revealed that an interwoven network involving more than a thousand reactions conduct the catabolic and anabolic activities of the cell (Bailey and Ollis, 1977). Moreover, the activities of enzyme catalysts necessary for cellular function are modulated at both the enzyme and gene level in response to environmental conditions. Further complicating this picture of cellular function is substantial evidence that metabolic activities vary with time in a controlled fashion during the course of the cell cycle (Mitchison, 1971). Thus, an individual cell is an extremely complicated, adaptive, yet programmed, chemical reactor.

Although current knowledge of molecular biology is extremely useful in developing desirable organisms for industrial microbial processes, not enough is known about the dynamics of molecular events and the complete array of interactions among molecular entities in the cell to permit calculations of cell growth rates or rates of product synthesis based on molecular models. Kinetics averaged over a single cell represent the next level of approximation, with averages over an entire population the coarsest possible focus.

Experimental measurements are relatively straightforward in the population-averaged situation. For example, it has been possible for some time to measure changes in cell mass concentration via optical density. However, it has been already widely recognized that knowledge of cell concentration alone is inadequate in general for representing the kinetics of cell growth, substrate utilization, and product formation in fermentation systems. Consequently, there have been efforts to develop structured models, that is, models which contain information on population average cell composition, for use in design and analysis of fermentation processes (Fredrickson et al., 1967; Malek et al., 1969). This approach has the advantage that, because one is analyzing properties averaged over an entire population, large samples are available, and a broad class of analytical methods can be brought to bear in experiments.

However, the population-averaged perspective does not recognize that different cells in the population may have different compositions and sizes. According to cell cycle research (Mitchison, 1971), cells of different ages likely contribute in much different ways to the overall behavior of the microbial system. This prompts an effort to understand the behavior of individual cells in the population during the fermentation process.

Observations of unstructured, that is, with no composition information, cell population statistics and dynamics have been possible for some time. In several previous studies, a Coulter counter or related apparatus has been used to determine the cell volume distribution. Examples of this class of investigations include the studies of Harvey, Marr, and Painter (1967) of *Escherichia coli* and *Azotobacter agilis*, Aiba and Endo (1971) on *Azotobacter vinelandii*, and Kothari et al. (1972) on *Schizosaccharomyces pombe*. In all of these studies, the underlying (individual) cell volume or mass growth rate was examined.

The Coulter counter approach for determining cell size distributions is not adaptable to measurement of single-cell composition, and as Harvey, Marr, and Painter (1967) observe, "our (size distribution) results do not give information about the kinetics of synthesis of cell material." Clearly, such information is desirable. As in the case of population-averaged kinetics, design equations which incorporate even a very simplified representation of cell physiology should be much more reliable for scale-up and other extrapolations than methods which employ only a single variable such as cell volume to characterize the microbial phase.

Another motivation for determining cell composition distributions in microbial populations are possible inadequacies in cell size as the most valuable single parameter for cell characterization. For example, in his presentation of a maturity-time representation for cell population dynamics, Rubinow (1968) states that "if the cell population is not homogeneous (which is surely always the case in a fermentation process) . . . only observation of intrinsic cellular properties is a true measure of maturation level." Cellular DNA content is suggested in the same work as an indicator of maturity of bacterial cells.

Also, knowledge of the cell composition distribution may be of direct value in certain special cases as one measure of the quality of the fermentation product. For example, in manufacture of single-cell protein, the ratio of protein to nucleic acid is an important parameter. Relatively high values of this ratio indicate a reduced danger of uric acid poisoning. It may be important to observe this protein/nucleic acid ratio in individual cells to determine if fermentation conditions or separation processes could be modified to increase the fraction of desirable cells in the final product.

Finally, measurements of the changes in cell composition distribution with time during batch growth and with dilution rate in continuous fermentation will provide new basic insights into microbial physiology and ecology, valuable in their own right. Even a pure bacterial submerged culture may be viewed as a mixed population in which young cells and old cells and small and large cells influence each other through their interaction with their common environment. More rapidly growing midcycle cells, for example, presumably contribute to nutrient exhaustion more than do slower growing smaller cells. Acids and other metabolic end products released into the medium by one segment of the population can alter the growth rates and metabolic processes of all members of the population. Information on the cell composition distribution can only enhance understanding of these types of interactions.

While the desirability of measuring the composition of individual cells has been clear for some time, only recently has instrumentation been developed which permits such data to be conveniently and rapidly amassed. The basic principles and features of this experimental technique are outlined next.

BASIC PRINCIPLES OF FLOW MICROFLUOROMETRY

Development of flow systems in which quantitative photometry is employed to measure cell characteristics started in 1965 (Kamentsky et al., 1965) and has since been continued in several laboratories in the United States and Germany (Van Dilla et al., 1969; Hulett et al., 1969; Springer et al., 1971; Dittrich and Göhde, 1969). The basic features of all of these instruments are similar. A schematic diagram of the University of Houston flow

microfluorometer (FMF) is shown in Figure 1. This unit is patterned closely after the Los Alamos instrument described in detail by Steinkamp et al. (1973).

In order to use the FMF to examine microbial populations, cells are withdrawn from the fermentation vessel and fixed. Formalin or aqueous solutions of methanol or ethanol may be employed for this pupose. Cells are then stained with fluorescent dyes which, in addition to specificity for certain cellular components, must also strongly absorb light at the available exitation wavelengths of a ½ W continuous argon laser (~488 nm). Stains for nucleic acids which approximate well these ideal characteristics are acriflavin used in conjunction with the Fuelgen reaction (see Culling and Vassar, 1961) and the intercalating dye propidium iodide (PI) (Hudson et al., 1969). A useful protein specific fluorescent dye is fluorescein isothiocyanate (FITC) (Udenfriend, 1969). Since maximum fluorescent emission occurs at different wavelengths for FITC (near 530 nm, blue-green) and the nucleic acid stains (near 590 nm for PI, orange-red), cells dyed with both dyes will emit distinguishable colored fluorescence. The intensities of the two-color emissions provide direct measures of cellular nucleic acid and protein content.

Such data are obtained in a flow microfluorometer as the cells in dilute suspension pass in free liquid stream through the laser beam. Typically, each cell is exposed to the laser light for a few microseconds, so that fluorescence decay difficulties are ameliorated. Two-color fluorescence detection is accomplished with a dual photomultiplier tube (see Figure 1 and Steinkamp et al., 1973). The resulting signals are processed electronically and stored on a multichannel pulse height analyzer.

Cells may flow through the instrument at rates of the order of 3 000/s, permitting examination of large numbers of cells in a relatively brief period. The accumulated information then provides useful statistics on the distribution of compositions within the cell population from which the sample was originally withdrawn.

BATCH BACTERIAL CULTIVATION: EXPERIMENTAL METHODS AND MATERIALS

An inoculum consisting of 100 ml of midexponential phase bacterial cells (*Bacillus subtilis* ATCC 6051a) was added aseptically at time zero to 2 500 ml of sterile medium in a 5 l fermentor jar. The same medium, consisting of 1.5 g KH_2PO_4, 1.5 g Na_2SO_4, 1.5 g NaCl, 0.15 g $MgSO_4 \cdot 7H_2O$, 0.45 g $CaCl_2 \cdot 6H_2O$, 0.013 g ferric citrate, 0.01 g $MnCl_2 \cdot 4H_2O$, and 2.5 g peptone/l water, and 2% (wt) glucose was used for inoculum growth and the subsequent fermentation. The inoculum was grown at 37°C with no *p*H control, while the following batch fermentation studied here was conducted at 37°C with *p*H maintained at 7.0 by controlled addition of acid and base. Sterile air was sparged into the fermentor at a rate of 0.8 vvm (volume of gas per volume of liquid per minute) through a single orifice immediately below a six-bladed paddle impeller rotated at 700 rev/min.

Starting 4 hr after inoculation and proceeding over the next 9 hr, samples of approximately 20 to 50 ml were withdrawn aseptically from the fermentation vessel each hour, and sample optical density at 420 nm was determined on a Coleman model 46 spectrophotometer. Culture purity was verified periodically throughout batch growth by plating a portion of the sample on nutrient agar (Difco). Centrifuged cell pellets were resuspended in 70% ethanol fixative, rinsed, and stained with FITC, PI, or both prior to analysis by the FMF. Composition distributions so determined were recorded photographically from the CRT display of the multichannel pulse height analyzer.

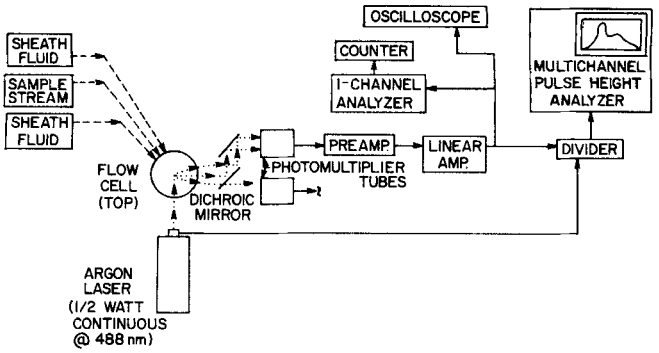

Fig. 1. Schematic diagram of the flow microfluorometer showing the signal processing sequence for one-color fluorescence measurements. Dashed, dotted, and solid lines denote fluid, light, and electronics signal flows, respectively.

EXPERIMENTAL RESULTS: ONE-COLOR FLUORESCENCE

Figure 2 shows the growth curve for the time period considered in this experiment. With little perceptible lag, the bacterial population grows at an exponential rate for approximately 5 hr. Over the next 5 hr, the culture enters a stationary phase which lasts for the balance of this experiment. Future experiments of longer duration will explore population changes during stationary and subsequent phases in greater detail. Emphasis in this work is on composition distributions and their changes during these initial growth phases.

Changes with time in the protein and nucleic acid distributions of the microbial population are shown in Figures 3, 4, and 5. A few words of explanation regarding the format of data presentation will facilitate subsequent discussion. All data shown are complete and unedited; the origin of each datum plot is indicated by the horizontal pointer in the lower left-hand corner of each part of the figures. The abscissa is relative protein content (FITC fluorescence) in parts a, b, c and relative nucleic acid content (PI fluorescence) in parts d, e, and f of each figure, and the ordinate is the relative number of cells with the indicated protein or nucleic acid content. The patterns of relatively less and more dense regions along the curves have been produced by manipulation of the CRT display in order to facilitate comparisons of mode locations and other shifts in the observed distributions.

The scattered points appearing in each plot for protein and nucleic acid contents near zero are results of

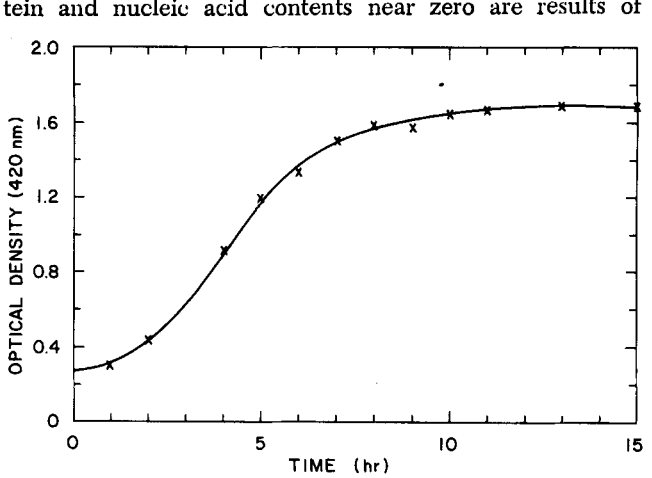

Fig. 2. Growth curve for batch cultivation of the bacterium *Bacillus subtilis*.

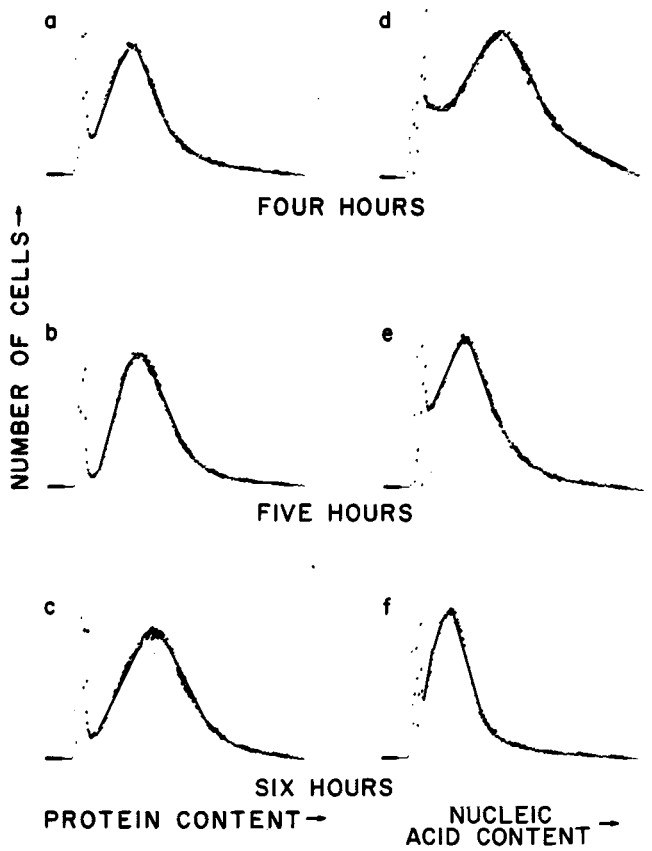

Fig. 3. Sequences of protein and nucleic acid distributions for hours four through six of the fermentation.

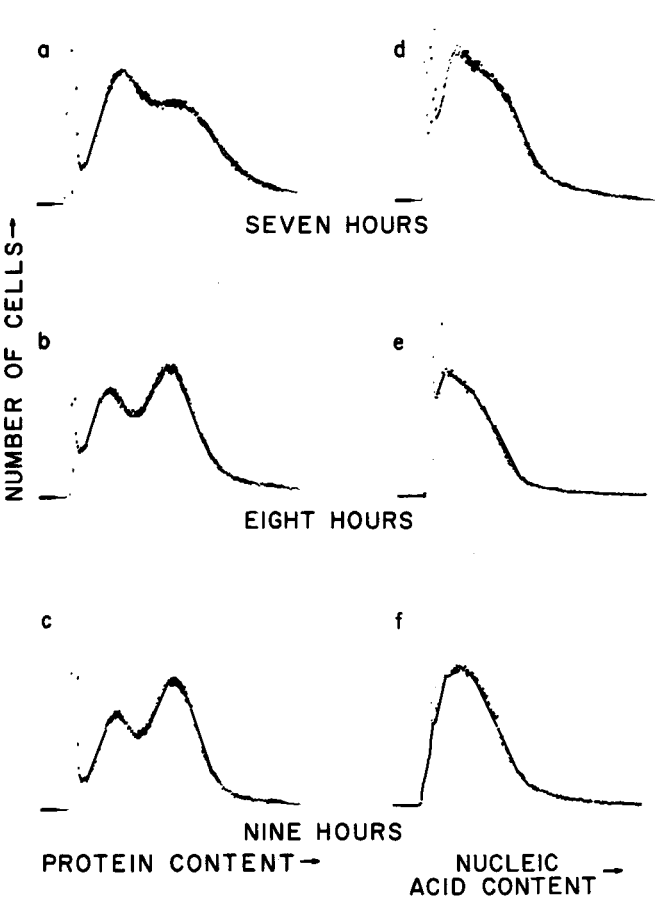

Fig. 4. The protein and nucleic acid distributions 7 through 9 hr after inoculation clearly reveal the presence of two subpopulations which are single vegetative cells and *Bacilli* chains.

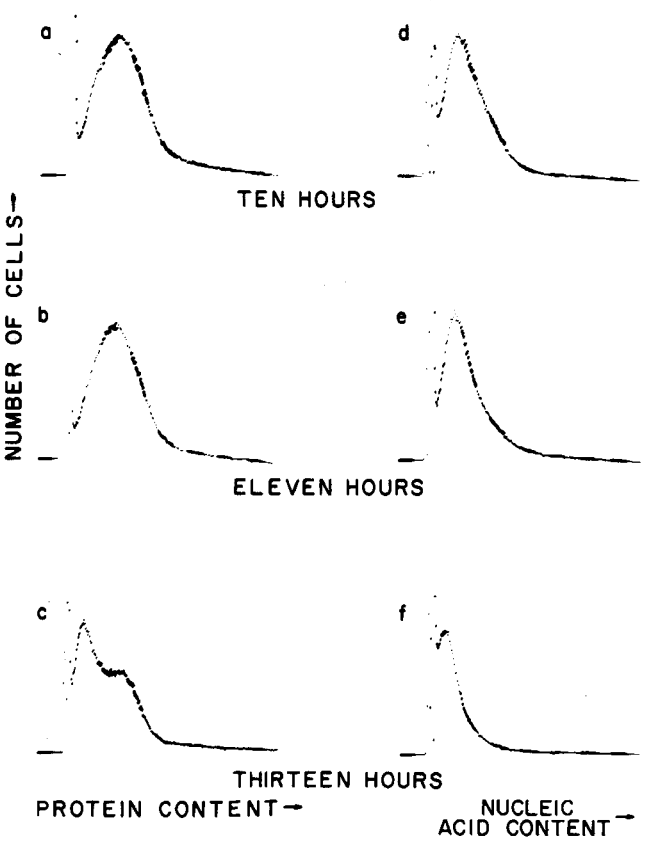

Fig. 5. The protein and nucleic acid distribution for hours ten through thirteen. Chains are not indicated in the FMF one-color data for 10 and 11 hr. The 13 hr protein distribution is bimodal due to the presence of endospores as well as vegetative cells at this stage of microbial growth.

electronic and optical noise and background fluorescence. Separation of individual bacterial cell fluorescence signals from this noise is a nontrivial problem whose solution requires optimal sample preparation and instrument adjustment. In most of these figures, it is evident where noise ceases and meaningful data begin.

The first sample was taken from the fermentor 4 hr after inoculation, and both the protein and nucleic acid distributions at this time reveal interesting features (Figures 3a, d). The protein data show a discontinuity in slope to the left of the mode, indicating that this distribution is likely the sum of two underlying distributions, presumably one at smaller protein levels comprised of endospores remaining from the inoculum and another at relatively larger protein contents resulting from vegetative cells. The broad nucleic acid distribution observed here in midexponential phase has a substantially larger mean and mode than is observed 2 hr later (Figure 3e). Except for a proportionality factor relating PI fluorescence to amount of nucleic acid, the means of these distributions correspond to classical measurements of average nucleic acid per cell. In this regard the pattern of change in Figures 3d, e, and f is consistent with previous measurements, indicating that early to midexponential phase bacterial cultures characteristically have, on the average, larger cells with higher nucleic acid content than cells later in the batch culture (see, for example, Herbert, 1961).

The slope discontinuity in the leading edge of Figure 3a is absent after an additional hour of growth (Figure 3b), but 6 hr after inoculation (Figure 3c), the protein distribution is widening. This development evolves into clearly bimodal protein distributions in Figures 4a, b, and c, a pattern which is echoed, albeit in a less obvious

fashion, in the corresponding nucleic acid distributions on Figure 4d, e, and f.

Microscopic examination of these samples and those preceding and following this period of bimodality reveal that between 7 and 9 hr after inoculation, two-membered chains of bacteria are found in considerable numbers in the microbial reactor. These chains, which are reflected in the FMF data by the modes furthest from the origin, are not unexpected. The bacterium employed in this study is a rod shaped microorganism which elongates as it grows. As binary fission occurs, a septum and ultimately a fully developed pair of membranes is synthesized which divides the parent cell into two daughter cells. Depending on environmental conditions, the daughter cells may separate quickly after this division is completed, or they may remain attached as occurred here between hours seven and nine. In some situations the daughter cells may remain together for several division cycles, leading to long chains of connected bacteria. Such long chains have not constituted a significant fraction of the biological population in any fermentation experiments so far conducted in the authors' laboratories.

Small bacilli chains are no longer apparent 10 hr after inoculation (Figures 5a, d), but a different type of bimodal distribution emerges after 13 hr as the microbial population moves further into the stationary phase (Figures 5c, f). Notice that the first mode in the protein distribution occurs at a much smaller protein content than in any of the other figures and that, with the maximum sensitivity available in these one-color fluorescence experiments, only a single mode can be seen in the 13 hr nucleic acid distribution.

Explanation of these results requires another brief digression into bacterial physiology. Several strains of bacteria, including the one investigated here, possess a defense mechanism against hostile environments such as those encountered during the stationary phase of batch growth. In an elaborate process, endospores, which are inactive forms of the bacteria, are synthesized. Endospores are smaller than vegetative cells, and they contain a complete bacterial chromosome which is protected by a surrounding multilayered coat of protein. In this form no growth occurs, but, on the other hand, the spore is capable of surviving extremes in temperature and other environmental conditions which would kill biologically active vegetative cells. If returned to a favorable environment, endospores germinate to yield normal, active vegetative bacteria.

The very sharp peak in Figure 5c is due to endospores, and the following plateau is the FMF manifestation of vegetative cells which remain in the population.

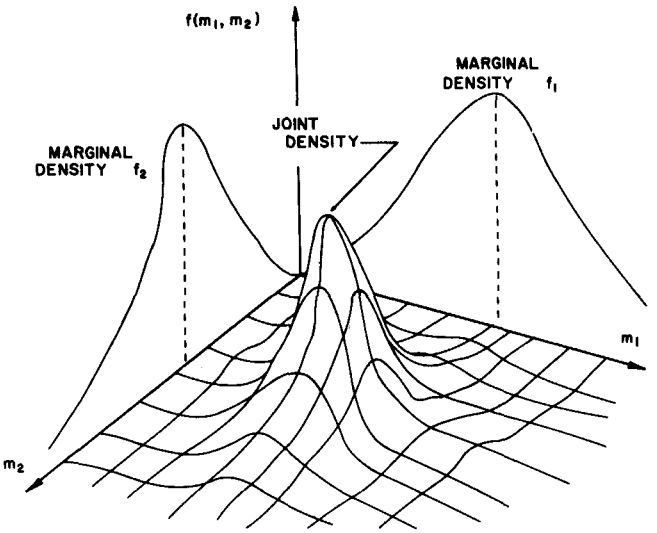

Fig. 6. Schematic diagram of the joint and marginal population densities, where in these experiments m_1 and m_2 correspond to cellular nucleic acid and protein content, respectively. The two-color fluorescence data displayed in Figures 8 and 9 are experimental approximations to sections of the joint density surface taken at various protein contents (m_2 values).

The nucleic acid distribution in Figure 5f is believed due entirely to the relatively small vegetative cells which are present at this point of the stationary phase. Spore nucleic acid fluorescence could not be distinguished from noise in these one-color fluorescence studies.

Summarizing these observations of the one-color fluorescence FMF data, it is clear that this experimental approach provides new insights into a number of significant physiological events: Figure 3a → 3b, completion of spore germination from the inoculum; Figure 3d → 3e, reduction in the average cellular nucleic acid content and in the dispersity of the nucleic acid distribution; Figure 5b → 5c, sporulation. Furthermore, morphological changes in the bacterial population are unmistakably apparent in the sequence of composition distributions observed from 6 through 10 hr after inoculation.

Especially noteworthy are the clearly visible shifts in composition distributions obtained on the FMF (see Figure 5), while classical, unstructured growth data (Figure 2) provide little evidence of important changes during the stationary phase. Since many commercially important enzymes and antibiotics are produced in the stationary phase of batch fermentations, FMF observations of population dynamics may provide improved understanding of process behavior leading ultimately to new design or operational strategies.

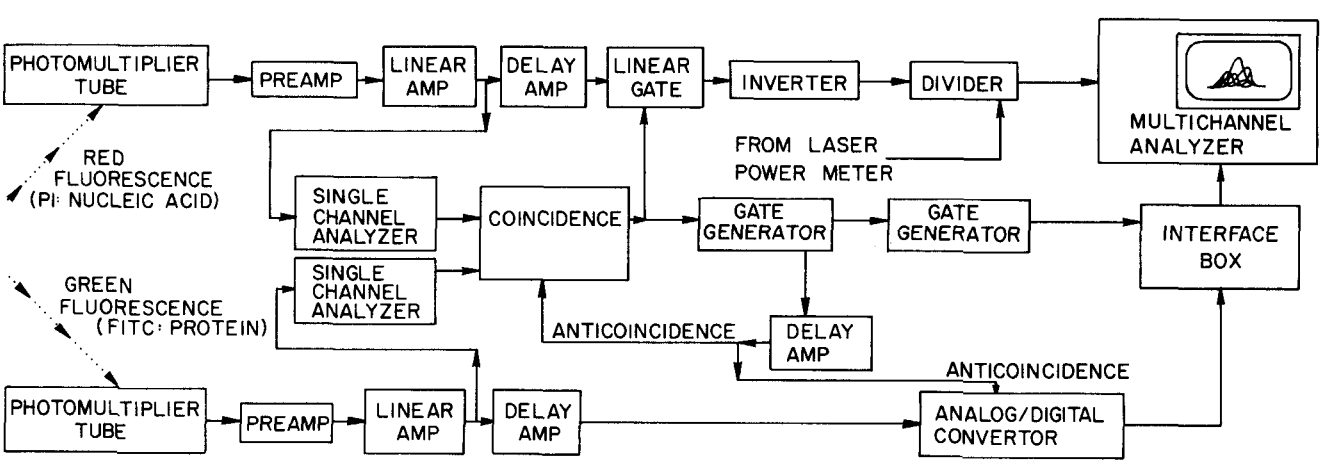

Fig. 7. Schematic diagram of signal processing electronics for two-color fluorescence measurements.

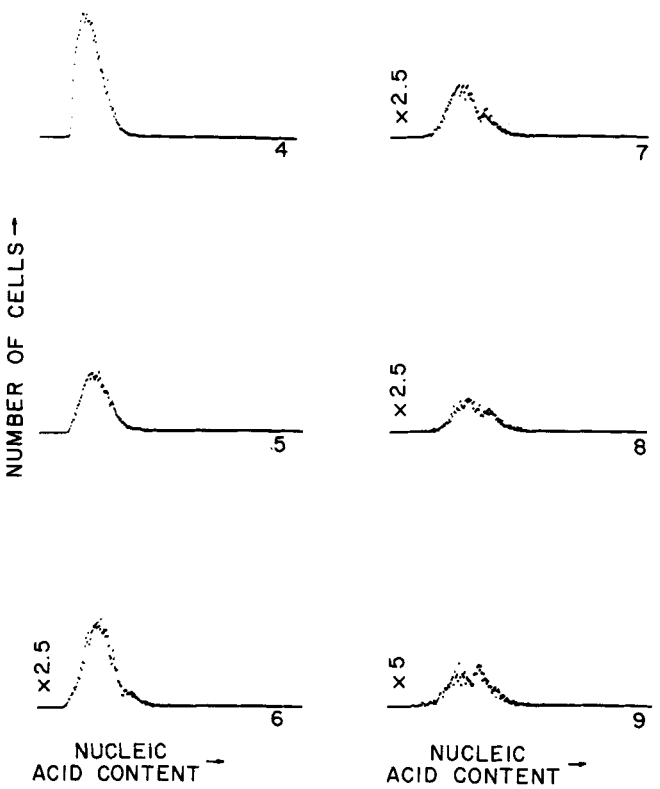

Fig. 8. Two-color fluorescence data for the microbial population 6 hr after inoculation. Numbers by various curves indicate channel number (= relative protein content) corresponding to each nucleic acid distribution.

It should be emphasized that the dynamics of population protein statistics are distinct from those for nucleic acid, indicating that access to both types of composition distributions adds significant information on population structure. In fact, knowledge of the joint protein-nucleic acid population density should be far superior to having the two one-dimensional protein and nucleic acid distributions separately.

EXPERIMENTAL RESULTS: TWO-COLOR FLUORESCENCE

For two-color fluorescence experiments, samples were stained with both PI and FITC. Subsequently, nucleic acid and protein contents of individual cells in the sample were determined simultaneously by the FMF. Accumulated data of this type provides a good experimental approximation to the joint population density $f(m_1, m_2)$, where $f(m_1,m_2)dm_1dm_2$ is the fraction of the population with nucleic acid contents between m_1 and $m_1 + dm_1$ and protein contents between m_2 and $m_2 + dm_2$. As Figure 6 depicts schematically, this density function may be viewed geometrically as a three-dimensional surface. Display of such a surface on these two-dimensional pages takes several possible forms, each containing significant information.

Two relatively straightforward forms of presentation are the marginal density functions:

$$f_1(m_1) \triangleq \int_0^\infty f(m_1, m_2)dm_2 \qquad (1a)$$

$$f_2(m_2) \triangleq \int_0^\infty f(m_1, m_2)dm_1 \qquad (1b)$$

Physically, $f_1(m_1)dm_1$ is the fraction of cells with nucleic acid contents between m_1 and $m_1 + dm_1$, while $f_2(m_2)dm_2$ has an analogous interpretation for protein. Except for abscissae scale factors and ordinate scaling to achieve normalization, the one-color data presented above are excellent approximations to the marginal densities.

Using the signal processing network illustrated in Figure 7, sections of the joint density function may be obtained and stored on a single multichannel pulse height analyzer. The essential purpose of the electronic system of Figure 7 is to select storage channel number based upon the fluorescence intensity of one color (FITC fluorescence in these experiments) and to accumulate the distribution of the second color fluorescence (here PI) in the selected channel. Mathematically, these sections are specified by

$$f_{1s,k}(m_1) = \int_{m_{2,k-1}}^{m_{2,k}} f(m_1, m_2)dm_2; \quad k = 1, 2, \ldots 16$$

$$m_{2,0} = 0 \qquad (2)$$

where $m_{2,k} - m_{2,k-1}$ = constant for all k, and where the $m_{2,k}$ grid is chosen to span the range of protein contents observed for the set of samples considered. Physically, $f_{1s,k}$ may be viewed approximately as the distribution of nucleic acid contents for cells with constant protein content of approximately $m_{2,k}$. To the same degree of approximation, $f_{1s,k}$ is geometrically the intersection of the joint density function surface with a plane orthogonal to the m_2 axis (see Figure 6) and intersecting the m_2 axis at approximately $m_{2,k}$. The index k will sometimes be referred to as channel number in reviewing the following experimental data, since operationally the sixteen nucleic acid distributions for various protein contents are stored in the sixteen different channels of the FMF multichannel pulse height analyzer.

Figure 8 shows six of the $f_{1s,k}$ sections as measured by the FMF. Channel numbers are indicated in the lower right-hand corner of each datum set, and the numerals written vertically are the relative gains of the ordinate display. Thus, for example, the ordinates of channels 5 and 9 should be divided by 2.5 and 5, respectively, before comparing those ordinates with ordinate values for channels 4 and 5.

The results in Figure 8 are for the microbial population after 6 hr of batch growth. At this point, the growth rate of the population has started to decrease from the maximal values observed 4 to 5 hr after inoculation. The 6 hr marginal protein and nucleic acid densities (see Figures 3c, f) show little or no indications of multiple subpopulations, although a bimodal pattern does emerge in the one-color data 1 hr later. In this context it is interesting that the 6 hr two-color data in Figure 8 exhibit bimodality in channels 7 through 9, and the irregularities in the slope of the descending region to the right of the modes in channels 5 and 6 are evidences of a substructure involving two different classes of individuals. This appearance of unusual structure in the nucleic acid distribution in the mid to high range of protein contents is presumably due to the presence of small numbers of chains of bacilli in this population.

This detail, which was not evident from the one-color fluorescence measurements, is accessible in two-color experiments for two different reasons. The first derives from the intrinsic relationship between marginal and joint densities; the latter suffers from less aggregation and therefore contains more information. Another factor enhancing sensitivity in two-color experiments is instrumental; the signal processing circuit of Figure 7 accepts information only when the two phototubes signals coincide. Since each phototube receives light of distinct wavelengths, the coincidence requirement minimizes accumulation of

spurious signals resulting from background fluorescence and other optical noise.

This enhanced sensitivity is even more dramatically apparent in the two-color data exhibited in Figure 9. These are the experimentally measured sections $f_{1s,k}$ for the bacterial population after 13 hr of batch growth. For this stationary phase population, endospores are indicated by the one-color protein data (Figure 5c) but not by the one-color nucleic acid data (Figure 5f). Nucleic acid fluorescence from spores is, however, apparent in the two-color measurements as evidenced by the bimodal nucleic acid distributions at relatively small protein contents (channels 2 and 3 in Figure 9). Subsequent experiments will include more extensive two-color studies in order to track the evolution of the joint population density during batch growth.

It should be noted that in all of the previous discussions and interpretations of FMF data, the identification of various peaks with corresponding subpopulations in the bacterial culture is based upon a reasonable synthesis of literature information, classical measurements, microscopic observations, and FMF experiments. The hypotheses so obtained should, of course, be subjected to direct experimental confirmation. This can be done by selecting a subpopulation based upon the fluorescence characteristics of its members and sorting cells possessing these properties from the remainder of the population. Addition to the FMF of appropriate logic elements for subpopulation selection and charged plates for droplet diversion can provide these capabilities (Hulett et al., 1969; Steinkamp, et al., 1973), and the University of Houston instrument is now being modified along these lines. Once full logic cell sorting is available, the subpopulations corresponding to different peaks and ridges in the marginal and joint population densities will be physically isolated and characterized by biochemical and microscopic analyses.

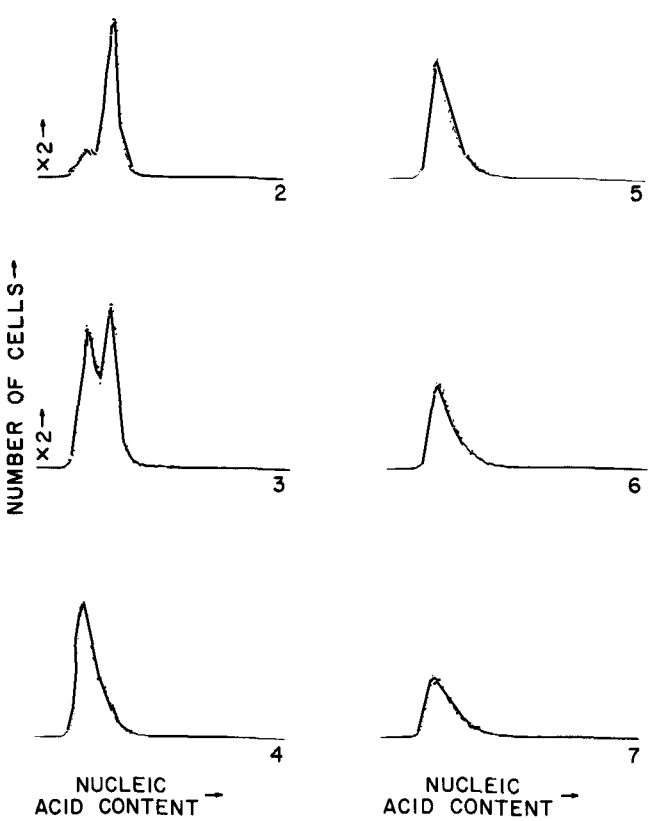

Fig. 9. The 13 hr two-color data exhibit bimodal nucleic acid content distributions for relatively small protein contents.

DISCUSSION

Formulation of mathematical models sufficiently robust to design microbial processes for operating conditions far removed from conditions used in determining the model has proven to be an extremely difficult and elusive goal. The experimental data presented above provide important new insights into the depths of this problem. Patterns of time evolution of the one-color composition distributions are extremely complex for protein, and a totally different sequence is observed for nucleic acid. The complicated state of bacterial population characteristics are further revealed in the two-color data. While Fredrickson et al. (1967) have formulated a very general structure for microbial population balance models, no specific models so far solved have produced results even remotely resembling these experimental data. It is now clear that substantially more complex models must be confronted in order to obtain a mathematical representation of microbial population behavior even qualitatively consistent with this new experimental reality. Nevertheless, there is cause for optimism. While flow microfluorometry has helped to clarify and reveal more fully the nature and magnitude of the challenge of modeling cell populations, it has likewise provided the data necessary to address the problem more directly. A logical first step in this direction seems to be application of FMF data from continuous culture to identfy the forms of the unknown rate and division density functions which appear in structured population balance equations. Such investigations are now in progress.

ACKNOWLEDGMENTS

The authors are indebted to Drs. John E. Evans, Allen H. Bartel, and John C. Allred for their assistance during this research. This work was made possible by generous financial support provided by the Camille and Henry Dreyfus Foundation, the University of Houston, and the National Science Foundation (NSF-RANN Grant No. APR75-13538). Any opinions, findings, or conclusions expressed herein are those of the authors and do not necessarily reflect the views of NSF.

NOTATION

f = joint population density
f_1 = marginal nucleic acid density
f_2 = marginal protein density
$f_{1s,k}$ = nucleic acid sections of the joint population density
m_1 = cellular nucleic acid content
m_2 = cellular protein content
$m_{2,k}$ = protein content grid points used in specification of the nucleic acid sections $f_{1s,k}$

LITERATURE CITED

Aiba, S., and I. Endo, "Statistical Analysis of Growth of Microorganisms," *AIChE J.*, **17**, 608 (1971).

Bailey, J. E., and D. F. Ollis, *Biochemical Engineering Fundamentals*, McGraw-Hill, New York (1977).

Culling, C., and P. Vassar, "Deoxyribose Nucleic Acid—A Fluorescent Histochemical Technique," *AMA Arch. Pathol.*, **71**, 88 (1961).

Fredrickson, A. G., D. Ramkrishna, and H. M. Tsuchiya, "Statistics and Dynamics of Procaryotic Cell Populations," *Math. Biosci.*, **1**, 327 (1967).

Fredrickson, A. G., R. D. Megee, III., and H. M. Tsuchiya, "Mathematical Models for Fermentation Processes," *Adv. Appl. Microbiol.*, **23**, 419 (1970).

Fredrickson, A. G., "Microbial Kinetics and Dynamics," in *Chemical Reactor Theory: A Review*, L. Lapidus and N. R. Amundson, ed., p. 405, Prentice-Hall, Englewood Cliffs, N.J. (1977).
Gaden, E. L., Jr., "Fermentation Kinetics and Productivity," *Chem. Ind.*, 154 (Feb. 12, 1955).
Harvey, R. J., A. G. Marr, and P. R. Painter, "Kinetics of Growth of Individual Cells of *Escherichia coli* and *Azotobacter agilis*," *J. Bacteriol.*, 93, 605 (1967).
Herbert, D., "The Chemical Composition of Micro-organisms as a Function of their Environment," *Symp. Soc. Gen. Microbiol.*, 11, 391 (1961).
Hudson, B., W. B. Upholt, J. Divinny, and J. Vinograd, "The Use of an Ethidium Analogue in the Dye-Buoyant Density Procedure for the Isolation of Closed Circular DNA: The Variation of the Superhelix Density of Mitochondrial DNA," *PNAS (US)*, 62, 813 (1969).
Hulett, H. R., W. A. Bonner, J. Barrett, and L. A. Herzenberg, "Cell Sorting: Automated Separation of Mammalian Cells as a Function of Intracellular Fluorescence," *Science*, 166, 747 (1969).
Kamentsky, L. A., M. R. Melamed, and H. Derman, "Spectrophotometer: New Instrument for Ultrarapid Cell Analysis," *ibid.*, 150, 630 (1965).
Kothari, I. R., G. C. Martin, P. J. Reilly, R. J. Martin, J. M. Eakman, "Estimation of Parameters in Population Models for *Schizosaccharomyces pombe* from Chemostat Data," *Biotechnol. Bioeng.*, 14, 915 (1972).
Malek, I., K. Beran, Z. Fencl, J. Ricica, H. Smrckova, and V. Munk, ed., *Continuous Cultivation of Microorganisms, Proc. 4th Symp.*, Academic Press, New York (1969).
Mitchison, J. M., *The Biology of the Cell Cycle*, Cambridge Univ. Press, London, England (1971).
Rubinow, S. I., "A Maturity-Time Representation for Cell Populations," *Biophys. J.*, 16, 1055 (1968).
Steinkamp, J. A., M. J. Fulwyler, J. R. Coulter, R. D. Hiebert, J. L. Horney, and P. F. Mullaney, "A New Multiparameter Separator for Microscopic Particles and Biological Cells," *Rev. Sci. Instrum.*, 44, 1301 (1973).
Udenfriend, S., *Fluorescence Assay in Biology and Medicine*, Vol. 2, Academic Press, New York (1969).
Van Dilla, M. A., T. T. Trujillo, P. F. Mullaney, and J. R. Coulter, "Cell Microfluorometry: A Method for Rapid Fluorescence Measurement," *Science*, 163, 1213 (1969).
Ward, H. M., "On the Biology of *Bacillus ramosus* (Fraenkel), a Schizomycete of the River Thames," *Proc. Royal Soc. (London)*, 58, 276, 288, 296, 461 (1895).

Manuscript received July 25, 1977; revision received December 19, and accepted January 6, 1978.

Prediction of Multicomponent Ion Exchange Equilibria for the Ternary System SO_4^{2-}-NO_3^--Cl from Data of Binary Systems

ROBERT P. SMITH
and
EDWARD T. WOODBURN
Department of Chemical Engineering
University of Natal
Durban 4001, South Africa

A framework is developed which provides predictions of multicomponent ion exchange equilibria from binary data.

Experimental data are reported for the ion exchange equilibria of the binary systems SO_4^{2-}-Cl^-, SO_4^{2-}-NO_3^-, and Cl^--NO_3^- on a strong base anion exchange resin. These systems exhibit nonideal characteristics in both phases, and the experimental characterization has been based on the reaction equilibrium constants and correlations for the activity coefficients in both phases. The exchanger phase activity coefficients are obtained from the well known Wilson (1964) model

The predictions of the ternary system SO_4^{2-}-NO_3^--Cl^- based solely on the binary data are consistent with the experimental data for this system.

SCOPE

The application of ion exchange in sorption operations is extensive. A major consideration preceding the implementation of this operation is the equilibrium distribution of ionic components between the solid and liquid phases for a particular system.

The aspects of thermodynamic equilibrium of ion exchange have been studied both theoretically and experimentally as reviewed by Helfferich (1962). More recently, Novosad (1973) studied the thermodynamics of ion exchange in the language of solution thermodynamics. Although a number of authors have investigated ternary systems (Klein et al., 1967; Streat and Brignal, 1970; Soldatov and Bychkova, 1971), the majority of published work is concerned with binary systems. This is limiting, since ion exchange is predominant in the fields of hydrometallurgy and water treatment which generally comprise complex multicomponent systems.

This work represents an attempt at the development of a framework from which the general, multicomponent, ion exchange system may be estimated.

The major hypothesis analogous to vapor-liquid equilibria is that the multicomponent system may be predicted from the combination of a number of subsystems that are characterized experimentally.

Correspondence concerning this paper should be addressed to Robert P. Smith, National Institute for Metallurgy, Private Bag X3015, Randburg, 2125, South Africa.